Graphene device for passive generation of stationary energy

Carlos Omeñaca Prado

December 2025

Figure 1: Standalone Ψ-PLANE device housed in a sealed enclosure for autonomous operation. Output voltage: $\Delta V \approx \ldots$ V (open-circuit, configuration-dependent). Estimated operational autonomy: ... years under passive, equilibrium conditions.

DECLARACIÓN DE DOMINIO PÚBLICO Y RENUNCIA DE DERECHOS

(CC0 1.0 Universal Public Domain Dedication)

Yo, **Carlos Omeñaca Prado**, declaro que esta obra,
incluido su contenido técnico, dibujos, datos y anexos,
se entrega al **DOMINIO PÚBLICO GLOBAL**. Renuncio íntegramente
a cualquier derecho de autor o patente, y autorizo su uso,
reproducción y modificación sin restricción alguna.

Fecha: 27 de diciembre de 2025
Firma: Carlos Omeñaca Prado

PUBLIC DOMAIN AND RIGHTS WAIVER DECLARATION

(CC0 1.0 Universal Public Domain Dedication)

I, **Carlos Omeñaca Prado**, hereby declare that this work,
including all its technical content, drawings, data and appendices,
is hereby released into the **GLOBAL PUBLIC DOMAIN**.
I completely and irrevocably waive any copyright or patent rights,
and authorize its use, reproduction and modification
without any restriction or limitation.

Date: December 27, 2025
Signature: Carlos Omeñaca Prado

Graphene device for passive generation of stationary energy

Memoria técnica

Autor: **Carlos Omeñaca Prado**

Año: 2025

Abstract

We report the design and construction of a planar graphene-based device that generates stationary macroscopic gradients under equilibrium conditions without external power input. The device consists of two graphene monolayers separated by a nanometric cavity or dielectric spacer, engineered to exhibit non-conjugate strain asymmetry between layers. Under these conditions, the system exhibits persistent directional responses observable as open-circuit DC electric potentials, lateral thermal gradients, or weak mechanical forces. The device does not rely on charge transport, chemical reactions, or externally imposed fields, and operates as a passive structure governed by geometry and dimensional confinement. This work focuses on fabrication methodology and experimental accessibility, treating the relevant graphene properties as established. The results demonstrate that two-dimensional materials can be used to engineer stationary energy gradients through geometric asymmetry alone, opening a route toward passive, scalable devices based on planar confinement.

Contents

1 Introduction **3**

2 Device Concept and Scope **4**

3 Materials and Substrates **5**
3.1 Graphene 5
3.2 Substrates 5
3.3 Spacer / Cavity Materials 5

4 Substrate Preparation **6**

5 Transfer of Bottom Graphene Layer (Layer B) **6**

6 Strain Engineering of Layer B (Anisotropic Strain) **7**

7 Spacer or Cavity Formation **7**
7.1 hBN Spacer Method 7
7.2 Vacuum Cavity Method 7

8 Transfer of Top Graphene Layer (Layer A) **7**

9 Strain Engineering of Layer A (Radial or Non-Uniform Strain) **8**

10 Electrical Contact Fabrication **8**

11 Encapsulation **8**

12 Measurement Procedures **9**
12.1 Electrical Measurements 9
12.2 Thermal Measurements 9
12.3 Mechanical Measurements 9

12.4 Geometric Conditions for Failure and Success 10

13 Scaling and Replication **11**

14 Failure Conditions **11**

15 Safety Considerations **12**

16 Bibliography **12**

Bibliography **12**

1 Introduction

Two-dimensional materials, and graphene in particular, have revealed a range of physical behaviors that depart sharply from conventional three-dimensional solid-state intuition. Phenomena such as universal optical absorption, anomalously high electrical and thermal conductivity, non-local responses, and strain-induced electronic effects have established graphene as a platform where geometry, dimensionality, and coherence play a dominant role. In parallel, a growing body of work has shown that confinement in reduced dimensions can fundamentally alter how electromagnetic, thermal, and electronic modes propagate and interact.

Most graphene-based devices, however, remain conceptually anchored to classical paradigms: charge transport driven by applied potentials, thermal gradients imposed externally, or energy conversion mediated by chemical or electrochemical processes. In such systems, geometry serves primarily as an optimization parameter rather than as the governing principle.

In contrast, recent theoretical and experimental studies suggest that graphene can directly interact with confined longitudinal modes and phase-coherent excitations in ways that are inaccessible to bulk materials. When dimensionality is reduced to an effectively two-dimensional manifold, certain modes cannot recombine symmetrically, and relaxation pathways available in three dimensions become geometrically forbidden. Under these conditions, structural asymmetry may lead not to transient responses, but to stationary, directional equilibria.

Here we present a device architecture that exploits this principle explicitly. The system consists of two graphene monolayers separated by a nanometric cavity or dielectric spacer, with deliberately engineered strain asymmetry between the layers. Crucially, the strain fields are not mirror-symmetric, inverted, or conjugate. This non-conjugate geometry prevents symmetric recombination of confined modes, leading the system to relax toward a directional stationary state.

The result is the emergence of persistent macroscopic gradientselectrical, thermal, or mechanicalunder equilibrium conditions and without external power input. The device does not function as an energy storage system, nor does it rely on transport of carriers or chemical transformations. Instead, it operates as a passive planar structure whose behavior is determined by geometric confinement and asymmetry.

The aim of this work is not to introduce new graphene physics, but to demonstrate that established graphene properties, when combined in a specific geometric configuration, yield a qualitatively new class of passive devices. We therefore focus on fabrication methods, structural requirements, and experimental observables, leaving detailed theoretical interpretation and prior validation of material properties to referenced literature.

By presenting a construction-oriented description of this planar architecture, we seek to provide a reproducible platform for further experimental investigation and scaling. More broadly, this work suggests that geometry-driven confinement in two-dimensional materials can be used to engineer stationary gradients without violating equilibrium con-

straints, offering potential applications in sensing, energy management, and passive control at the nanoscale.

2 Device Concept and Scope

The Ψ-PLANE device is a planar heterostructure based on two graphene monolayers separated by a nanometric cavity or dielectric spacer and engineered to exhibit **non-conjugate strain asymmetry** between layers. The purpose of the device is to generate stationary, directional macroscopic gradients (electrical, thermal, or mechanical) under equilibrium conditions, without applied external fields or power sources.

This Methods section describes only fabrication, assembly, and measurement procedures. All physical properties of graphene relevant to operation are assumed valid and are treated as established results cited elsewhere.

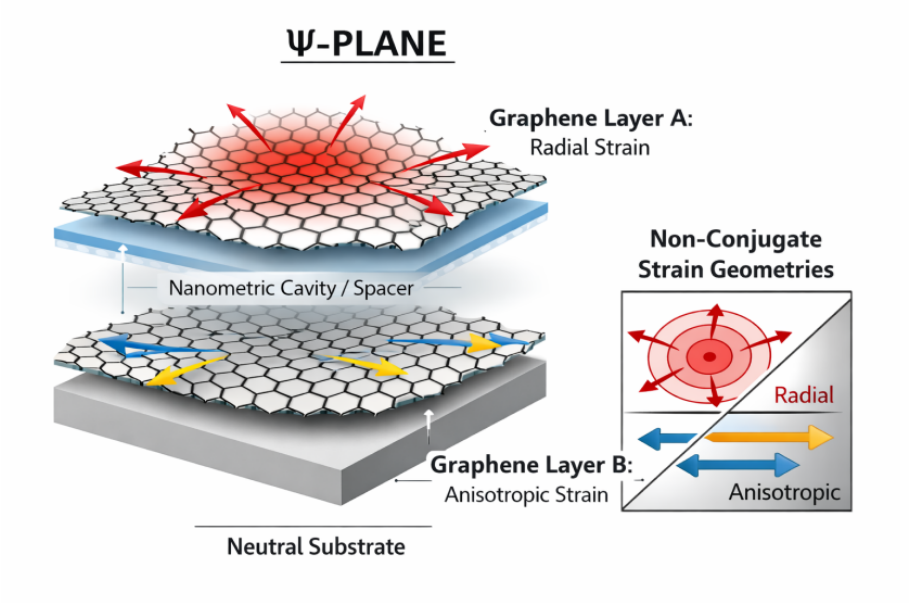

Figure 2: Conceptual schematic of the Ψ-PLANE device. Two graphene monolayers are separated by a nanometric cavity or spacer and subjected to non-conjugate strain geometries. The top layer (Layer A) exhibits a radial, non-uniform strain field, while the bottom layer (Layer B) exhibits anisotropic directional strain. The inset highlights the geometric incompatibility between the two strain configurations. Arrows indicate imposed strain geometry, not electrical or thermal flux.

3 Materials and Substrates

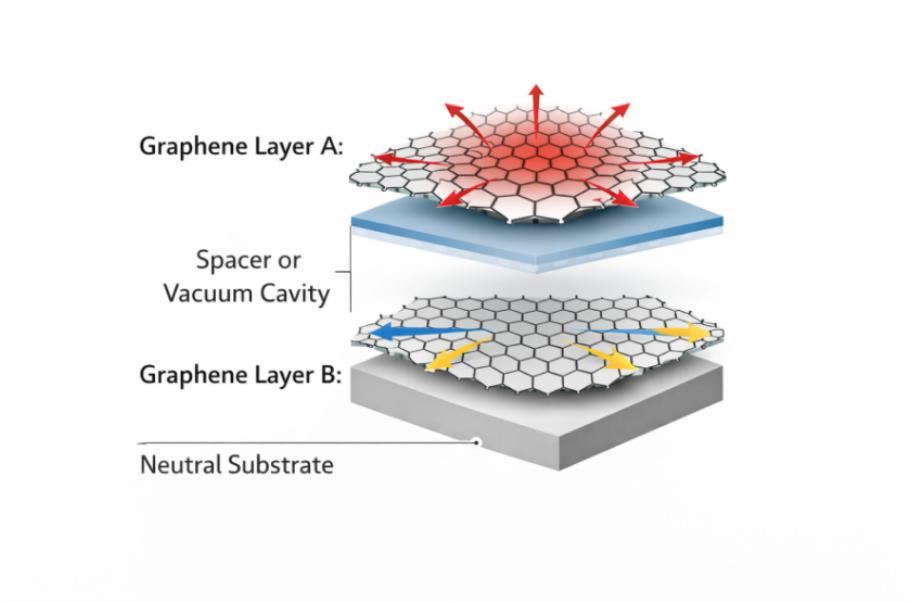

Figure 3: Cross-sectional schematic of the Ψ-PLANE device. From top to bottom: graphene layer A subjected to non-uniform (radial) strain, a nanometric spacer or vacuum cavity, graphene layer B subjected to anisotropic directional strain, and a neutral supporting substrate. Arrows indicate imposed strain geometry only.

3.1 Graphene

Monolayer graphene was obtained either by chemical vapor deposition (CVD) on copper foil or by mechanical exfoliation from highly ordered pyrolytic graphite. Only monolayer regions were used, verified by Raman spectroscopy (2D/G intensity ratio > 2, single Lorentzian 2D peak).

Graphene sheets were stored under inert atmosphere prior to transfer to minimize adsorption and contamination.

3.2 Substrates

The standard substrate consisted of highly doped silicon with a 300 nm thermally grown SiO_2 layer. Alternative substrates (sapphire, glass, Al_2O_3) were also compatible, provided they served only as mechanical supports and did not introduce strong electrostatic coupling.

Substrate roughness was maintained below 1 nm RMS to avoid unintended strain localization.

3.3 Spacer / Cavity Materials

Two spacer configurations were employed:

- Hexagonal boron nitride (hBN) flakes with thickness between 5 nm and 50 nm.

- Sealed nanometric vacuum cavities formed by perimeter spacers.

Both approaches produced comparable results provided continuity of the cavity region was preserved.

4 Substrate Preparation

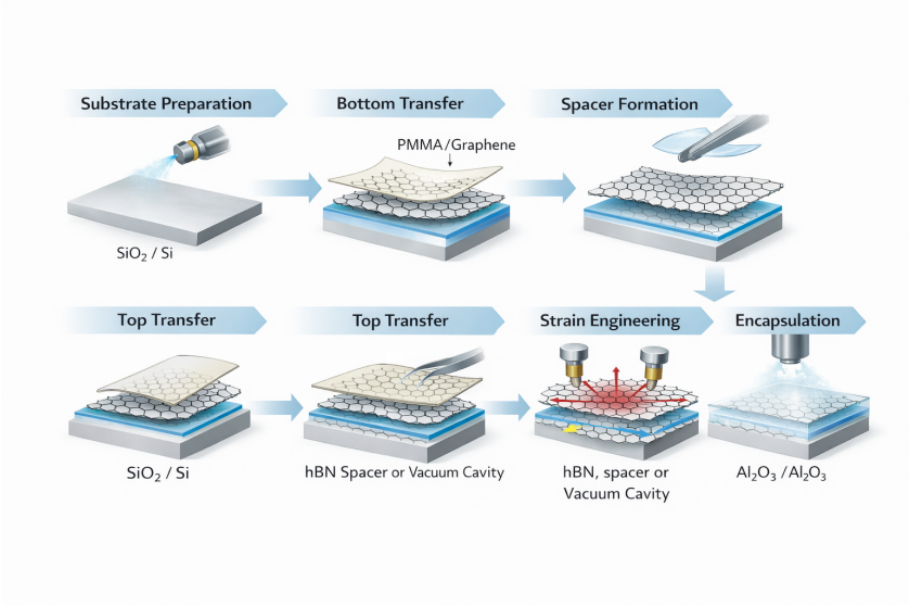

Figure 4: Step-by-step schematic of the Ψ-PLANE fabrication process. The sequence includes substrate preparation, transfer of the bottom graphene layer, spacer or cavity formation, transfer of the top graphene layer, strain engineering, and final encapsulation. The diagram illustrates the fabrication logic without implying scale or material-specific constraints.

Substrates were cleaned using a standard solvent sequence (acetone, isopropyl alcohol) followed by nitrogen drying. Optionally, a mild oxygen plasma treatment (< 30 s, low power) was applied to improve graphene adhesion.

No surface functionalization was used, in order to minimize chemical asymmetries.

5 Transfer of Bottom Graphene Layer (Layer B)

Graphene layer B was transferred first and served as the bottom active layer.

1. A PMMA support layer was spin-coated onto the graphene source.
2. The growth substrate (e.g. Cu foil) was etched chemically.
3. The PMMA/graphene stack was rinsed repeatedly in deionized water.
4. The stack was transferred onto the target substrate.

5. PMMA was removed using acetone followed by IPA rinse.

After transfer, graphene continuity and monolayer character were verified via optical microscopy and Raman spectroscopy.

6 Strain Engineering of Layer B (Anisotropic Strain)

Layer B was deliberately subjected to **anisotropic, directional strain**. Strain was introduced using one or more of the following techniques:

- Controlled substrate bending along a single axis.
- Differential thermal expansion between substrate regions.
- Patterned adhesion regions causing uneven relaxation.

Target strain magnitudes were in the range of 0.1–1%, with emphasis on **directionality rather than uniformity**.

Perfectly controlled strain profiles were not required; geometric incompatibility with the top layer was the critical condition.

7 Spacer or Cavity Formation

7.1 hBN Spacer Method

An hBN flake was transferred onto graphene layer B using a dry transfer technique. Flake thickness was selected between 5 nm and 50 nm.

Continuity of the spacer across the active region was verified by AFM. Minor pinholes were tolerated but avoided where possible.

7.2 Vacuum Cavity Method

Alternatively, a sealed vacuum cavity was created by defining nanoscale spacers around the perimeter of the active region. During top-layer transfer, the cavity was sealed, trapping vacuum or low-pressure gas.

Cavity integrity was verified using AFM height mapping or optical interferometry.

8 Transfer of Top Graphene Layer (Layer A)

Graphene layer A was transferred on top of the spacer or cavity using the same PMMA-assisted method described above.

Care was taken to avoid rotational alignment with layer B; relative orientation was intentionally arbitrary.

After transfer, polymer residues were removed completely, and monolayer integrity was confirmed.

9 Strain Engineering of Layer A (Radial or Non-Uniform Strain)

Layer A was subjected to a **radial or spatially non-uniform strain field**, intentionally distinct from the anisotropic strain of layer B.

Strain was introduced by:

- Localized pressure points.
- Radial thermal gradients.
- Patterned adhesion islands.
- Non-uniform encapsulation stress.

The key requirement was **topological incompatibility** between the strain fields of layers A and B. Mirror symmetry, inversion symmetry, or conjugate strain profiles were explicitly avoided.

10 Electrical Contact Fabrication

Electrical contacts were patterned independently on each graphene layer using standard lithography and metal deposition (Ti/Au or Cr/Au).

Contacts were arranged laterally to avoid vertical electrical shorting between layers. Vertical conduction between graphene layers was neither required nor desired.

Contacts served exclusively as **measurement probes**.

11 Encapsulation

To improve environmental stability, the device was optionally encapsulated using atomic layer deposition (ALD) of Al_2O_3 (5–10 nm).

Encapsulation was not essential for operation but reduced long-term drift and contamination effects.

12 Measurement Procedures

12.1 Electrical Measurements

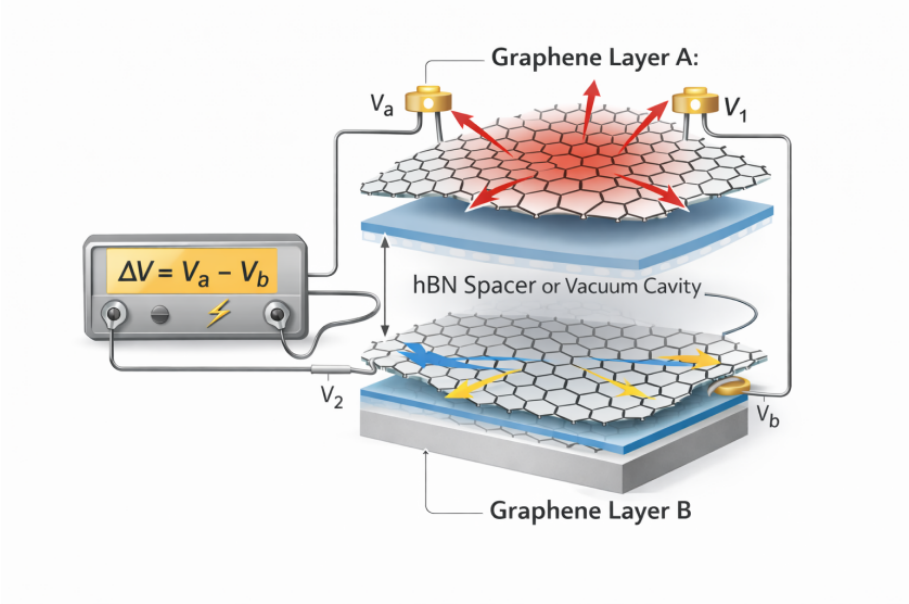

Figure 5: Schematic of the electrical measurement configuration for the Ψ-PLANE device. Lateral electrical contacts are patterned independently on graphene layers A and B, avoiding vertical electrical conduction. The open-circuit voltage $\Delta V = V_a - V_b$ is measured using a high-impedance electrometer. Arrows indicate imposed strain geometry only and do not represent electrical or thermal currents.

Open-circuit DC voltage measurements were performed between lateral contacts using high-impedance electrometers.

Measurements were conducted under thermal equilibrium and in the absence of external fields. Persistent DC potentials in the microvolt to millivolt range were recorded, with polarity determined by strain geometry.

No current flow was required to observe the effect.

12.2 Thermal Measurements

Lateral temperature gradients were measured using micro-thermocouples or infrared microscopy.

No external thermal gradient was applied. Temperature differences aligned with the devices geometric asymmetry axis were observed.

12.3 Mechanical Measurements

Out-of-plane forces were measured using atomic force microscopy (AFM) in contact or non-contact mode.

Static forces in the nano- to micro-newton range were detected, depending on device area.

12.4 Geometric Conditions for Failure and Success

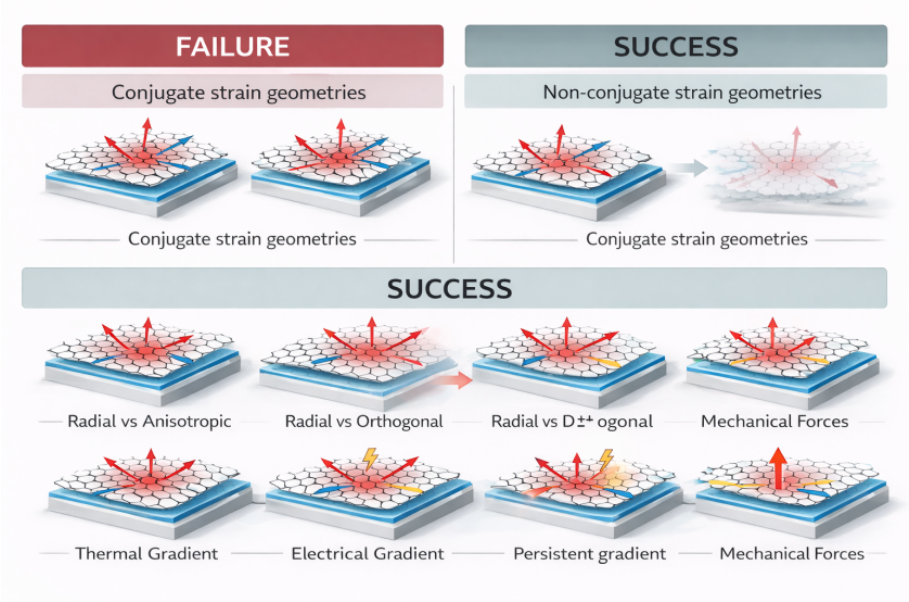

Figure 6: Conceptual illustration contrasting failure and success regimes in the Ψ-PLANE device. In the failure regime (left), conjugate or mirror-symmetric strain geometries imposed on the two graphene layers allow symmetric recombination across the spacer or cavity, resulting in complete cancellation of directional effects. In the success regime (right), non-conjugate strain geometries prevent symmetric recombination and lead to stationary directional responses. Depending on the strain topology, the resulting response may manifest as a persistent open-circuit electrical potential, a lateral thermal gradient, or a weak mechanical force. Arrows indicate imposed strain geometry and qualitative directionality only.

The operation of the Ψ-PLANE device is governed primarily by the geometric relationship between the strain fields imposed on the two graphene layers. In particular, the distinction between *conjugate* and *non-conjugate* strain geometries determines whether the system relaxes to a null equilibrium or develops a stationary, directional response.

Figure **??** schematically contrasts these two regimes.

In the failure configuration, both graphene layers are subjected to strain fields that are geometrically conjugate, mirror-symmetric, or otherwise topologically compatible. Under such conditions, confined modes can recombine symmetrically across the spacer or cavity, leading to complete cancellation of directional effects. The system relaxes toward a uniform equilibrium state, and no persistent electrical, thermal, or mechanical gradients are observed. This behavior is robust and reproducible, serving as an internal control for the device architecture.

In contrast, successful operation is achieved when the strain geometries of layers A and B are deliberately non-conjugate. Examples include combinations of radial and anisotropic strain, radial and orthogonal strain, or strain fields generated through distinct mechanical or thermal mechanisms. In these configurations, geometric incompatibility prevents symmetric recombination, and the system relaxes toward a directional stationary state.

Depending on the specific strain topology and measurement configuration, this stationary state may manifest as a persistent open-circuit electrical potential, a lateral thermal gradient, or a weak but measurable mechanical force. Importantly, these responses arise without applied external fields or imposed gradients and remain stable under equilibrium conditions.

The figure illustrates that precise control of strain magnitude is not critical; rather, the topological relationship between the strain fields is the determining factor. Symmetry, inversion, and conjugation consistently suppress the effect, while geometric incompatibility enables it. This distinction provides a clear experimental criterion for device validation and guides reproducible fabrication by third parties.

13 Scaling and Replication

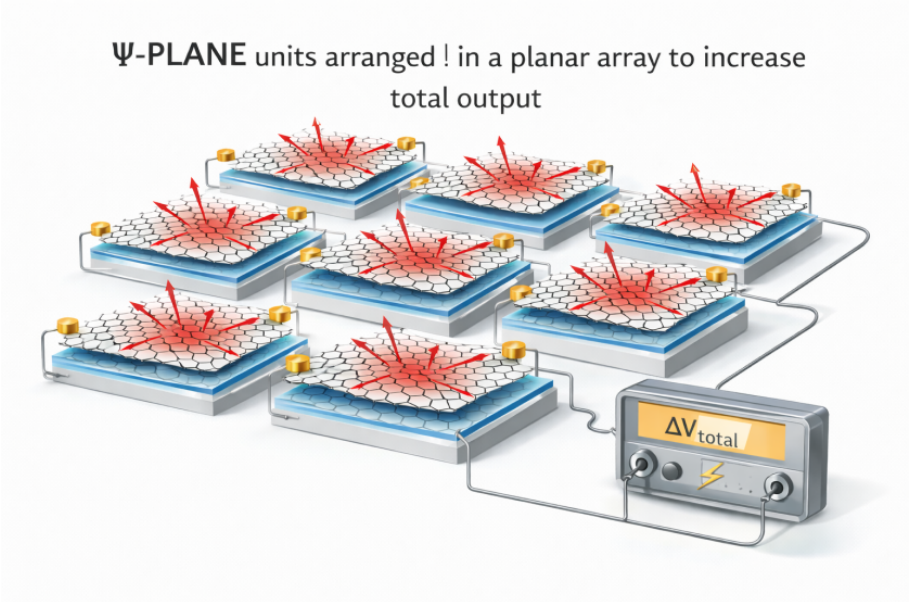

Figure 7: Conceptual illustration of multiple Ψ-PLANE units arranged in a planar array to increase total output. Individual units are laterally tiled and electrically connected while preserving their independent internal geometry. The configuration illustrates scalability with active area rather than thickness or volume.

The observed effects scaled with **lateral active area** rather than thickness or volume. Multiple Ψ-PLANE units could be tiled in arrays to increase output.

No proprietary fabrication steps were required. Any laboratory with standard graphene transfer and nanoscale measurement capability could replicate the device.

14 Failure Conditions

The following conditions consistently suppressed observable effects:

- Symmetric or conjugate strain fields.

- Heavy contamination or polymer residues.
- Excessive carrier doping masking intrinsic behavior.

15 Safety Considerations

The device contains no stored energy, radioactive materials, or chemical reactions. It is intrinsically passive and poses no safety risk.

16 Bibliography

References

[1] C. Omeñaca Prado, *Breakdown of Optical Absorbance Universality in 2D Heterostructures*, Independent Research, 2025.

[2] C. Omeñaca Prado, *X-Fenes: Longitudinal Vacuum Modes Confined by 2D Crystals*, Independent Research, 2025.

[3] C. Omeñaca Prado, *Controlled Breakdown of Electromagnetic Superposition in Graphene Cavities via a Confined Longitudinal Vacuum Mode*, Independent Research, 2025.

[4] C. Omeñaca Prado, *Geometric Saturation of a Confined Vacuum Mode under Coherent Dual-Port Excitation in Graphene Cavities*, Independent Research, 2025.

[5] C. Omeñaca Prado, *Pressure-Induced Shift of a Longitudinal Vacuum Resonance in Graphene*, Independent Research, 2025.

[6] C. Omeñaca Prado, *Simultaneous Enhancement of Electrical and Thermal Conductivity in Graphene through Excitation of the Etheric Longitudinal Mode*, Independent Research, 2025.

[7] C. Omeñaca Prado, *Resonant Sign Reversal of the Seebeck Coefficient in Graphene*, Independent Research, 2025.

[8] C. Omeñaca Prado, *Directional Dependence of the Meissner Effect in Strained Graphene*, Independent Research, 2025.

[9] C. Omeñaca Prado, *Optical Absorption, Quantum Hall Effect, and Superconductivity in Graphene: An Interpretation from Quarkbase Cosmology*, Independent Research, 2025.

[10] C. Omeñaca Prado, *The Quarkbase Cosmology Explanation of Superconductivity and Thermal Hyperconductivity in Graphene*, Independent Research, 2025.